EurJIC
European Journal of Inorganic Chemistry

Research Article
doi.org/10.1002/ejic.202400159

Chemistry Europe
European Chemical Societies Publishing

www.eurjic.org

Square-Planar Copper(II) complexes from a Zwitterionic Schiff-Base $N_2/N_{2/2}$-Donor Ligand: DNA Interaction and Cytotoxicity

Jordi Grau,[a] David Montpeyó,[b] Julia Lorenzo,[b] Olivier Roubeau,[c] Amparo Caubet,*[a] and Patrick Gamez*[a, d, e]

A new tetradentate ligand, namely 3,3′-((1*E*,1′*E*)-(ethane-1,2-diylbis(azaneylylidene))bis(methaneylylidene))bis(pyridin-2-amine) (**en2ampy**) was prepared and two copper(II) complexes, *viz.* [Cu(**en2ampy**)]Cl_2 (**1**) and [Cu(**en2ampy**)]$(NO_3)_2$ (**2**), were obtained through its reaction with copper(II) chloride and copper(II) nitrate, respectively. The single-crystal X-ray structure of the compounds showed that the metal centre was coordinated in a square-planar fashion by a doubly deprotonated **en2ampy** acting as a tetradentate N_2/N_2^{2-}-donor ligand. DNA-binding studies revealed that **1** and **2** were electrostatically binding to DNA, probably in the grooves and cytotoxicity assays showed that the complexes were clearly more efficient than cisplatin against ovarian carcinoma (A2780) cells and the cisplatin-resistant (A2780Cis) ones.

Introduction

Cancer is the second-leading cause of death in the world.[1] For instance, in 2022, about 20 million new cancer cases were reported and 9.7 million people died of this disease.[2] The World Health Organization (WHO) estimates that the number of new cancer cases will increase to more than 35 million in 2050.[2] Thus, this rapidly growing global cancer burden urgently requires the development of new efficient anticancer agents.[3] In that context, chemotherapeutic drugs based on metal complexes have increasingly gained interest[4] after the discovery of the anticancer properties of cisplatin, *i.e. cis*-diamminedichloridoplatinum(II), in 1965 by Rosenberg.[5]

Copper is an essential trace element in the human body;[6] its misbalance induces disorders such as Menkes disease, Wilson's disease, etc.[7] Because it is a bioelement, it is expected that copper-based compounds may be less toxic than other metal complexes, for instance containing metal ions from the platinum group.[8] Hence, copper complexes with potential anticancer activity have increasingly been reported.[9] Copper(II) complexes from Schiff base ligands represent an important family of compounds in this area of research,[10] some of them exhibiting remarkable cytotoxic activities.[11]

In the present study, a very simple and new N4-donor Schiff base ligand, *viz.* 3,3′-((1*E*,1′*E*)-(ethane-1,2-diylbis(azaneylylidene))bis(methaneylylidene))bis(pyridin-2-amine) (**en2ampy**; Scheme 1), was prepared from two commercially available reagents, namely ethylenediamine and 2-amino-nicotinaldehyde.

Two coordination compounds were then prepared by reaction of the ligand **en2ampy** with copper(II) chloride and copper(II) nitrate in ethanol. The copper(II) complexes, *i.e.*, [Cu(**en2ampy**)]Cl_2 (**1**) and [Cu(**en2ampy**)]$(NO_3)_2$ (**2**), were fully characterized and their X-ray crystal structures revealed that, unexpectedly, the **en2ampy** was acting as a tetradentate N_2/N_2^{2-}-donor ligand (*viz.*, two deprotonated amine groups were coordinated to metal centre). DNA-interaction studies showed that the two copper(II) compounds were establishing electrostatic contacts with the biomolecule. Although complexes **1**

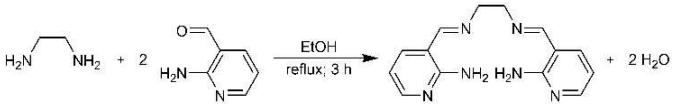

Scheme 1. Synthetic procedure for the preparation of the ligand **en2ampy**.

[a] *J. Grau, Dr. A. Caubet, Prof. P. Gamez*
nanoBIC, Department of Inorganic and Organic Chemistry
Universitat de Barcelona
Martí i Franquès 1–11, 08028 Barcelona, Spain
E-mail: amparo.caubet@qi.ub.es
patrick.gamez@qi.ub.es

[b] *Dr. D. Montpeyó, Dr. J. Lorenzo*
Institute of Biotechnology and Biomedicine "Vicent Villar Palasi" (IBB) and Department of Biochemistry and Molecular Biology
Universitat Autònoma de Barcelona
Parc de Recerca, Mòdul B08193 Bellaterra (Cerdanyola del Vallès), Spain

[c] *Dr. O. Roubeau*
Instituto de Nanociencia y Materiales de Aragón (INMA)
CSIC and Universidad de Zaragoza
Plaza San Franciscos/n, 50009 Zaragoza, Spain

[d] *Prof. P. Gamez*
Institute of Nanoscience and Nanotechnology (IN2UB), Universitat de Barcelona
08028 Barcelona, Spain

[e] *Prof. P. Gamez*
Catalan Institution for Research and Advanced Studies (ICREA)
Passeig Lluís Companys 23, 08010 Barcelona, Spain

Supporting information for this article is available on the WWW under https://doi.org/10.1002/ejic.202400159

Research Article
doi.org/10.1002/ejic.202400159

and **2** are not DNA-cleaving agents, they are significantly cytotoxic, with IC_{50} values in the low micromolar range for the two cell lines tested.

Results and Discussion

Crystal Structures

Single crystals of both complexes could be obtained, which were analyzed by X-ray diffraction. Crystal data and structure refinement parameters are listed in Table S1, and selected bond distances and angles are given in Table S2.

Complex **1** crystallizes in the triclinic space group $P\bar{1}$ (Table S1). A representation of its solid-state structure is shown in Figure 1. The copper(II) complex exhibits a square-planar coordination geometry formed by four N-donor atoms from the ligand **en2ampy**. Surprisingly, **en2ampy** acts as a doubly amine-deprotonated ligand, the two protons been transferred to the vicinal pyridine rings, as depicted in Scheme S1. Amido ligands, *i.e.* R_2N^-, represent an interesting class of ligands; for instance, they have been used with second-row transition metals (*e.g.*, ruthenium,[12] rhodium,[13] gold,[14] or iridium[15]) to activate coordinated substrates.[16] Examples of amido ligands with first-row transition metal ions are comparatively scarcer. Bulky (trialkylsilyl)amido ligands of the type LiN(SiPr$^i_3$)Dipp (Dipp = 2,6-diisopropylphenyl) are usually employed to generate low–coordinate complexes of first-row transition metals,[17] including copper.[17e,18] For example, a two-coordinate copper(II) complex of formula Cu{N(SiMe$_3$)}Dip$_2$ was first described with its crystal structure in 2016.[18] The coordination of simple deprotonated amines to copper has not been frequently described in the literature; in 2009, a three-coordinate copper(I) amido complex containing a deprotonated 4-methyl-*N*-(4-methylphenyl)aniline (*i.e.*, deprotonated di-*p*-tolylamine) was reported.[19] Subsequently, several examples of related three-coordinate copper(II) complexes were published, which showed interesting catalytic properties.[20] Amido ligands with carbene-type complexes have also been described, for instance with deprotonated aniline, like in the copper(I) complex of formula [(IPr)Cu(NHPh)] (with IPr = 1,3-bis(2,6-diisopropylphenyl)imidazol-2-ylidene).[21]

In our case, the type of amido ligand appears to be unprecedented. First, it is a chelating bis-anilido-containing system obtained from a simple Schiff base acting as both an N_2- and N_2^{2-}-donor set. Obviously, the basicity of the neighbouring pyridine moieties facilitates the deprotonation of the $-NH_2$ groups. Hence, **en2ampy** coordinates the metal centre in a zwitterionic form (Scheme S1), generating a (flat) square-planar complex where the copper(II) charge is balanced by the two N^- atoms (Figures 1 and S1). The positive charges on the pyridinium rings of the metal complex are counter-balanced by two lattice chloride anions. It can be pointed out here that the chloride anions, which are considered to be coordinating ions, are not bonded to the metal centre, suggesting that the tetradentate N_2/N_2^{2-}-donor unit acts as a strong ligand, generating a stable square-planar copper complex. The coordination angles vary from 83.7(2) to 93.6(2)°; the lowest angle of 83.7(2)° arises from the coordination of the rigid bis-diimine unit of the ligand (*i.e.*, N3-Cu1-N4 angle). The Cu–N bond distances are in the range 1.924(5)–1.977(5) Å (Table S2). It can be noted that the anilido-copper bonds of 1.933(5) and 1.924(5) Å are shorter than the imine-copper ones. These values close to 1.9 Å confirm that the amine moieties are deprotonated,[20a,21] the Cu–N distances for a $-NH_2$ group expected to be close to 2 Å.[22]

The crystal packing of **1** exhibits some interesting features. First, each cationic part of **1** is hydrogen bonded to another cationic unit through two chloride anions, as illustrated in Figure 2. Hence, one of the pyridinium moieties of the cationic unit [Cu(**en2ampy**)]$^{2+}$ is involved in the bonding with two chlorides (Cl1) while the other pyridinium (N2-H2) is interacting with a lattice water molecule (O1w). Moreover, the remaining hydrogen atom of the anilido group (N6-H6) is also interacting with the chloride anion (Table S3).

These hydrogen-bonded dimers are packed along the crystallographic *a* axis, generating stacks of [Cu(**en2ampy**)]$^{2+}$ cations that are separated by supramolecular assemblies between the lattice water molecules and chloride anions (Figure S2). The supramolecular water-chloride chains are

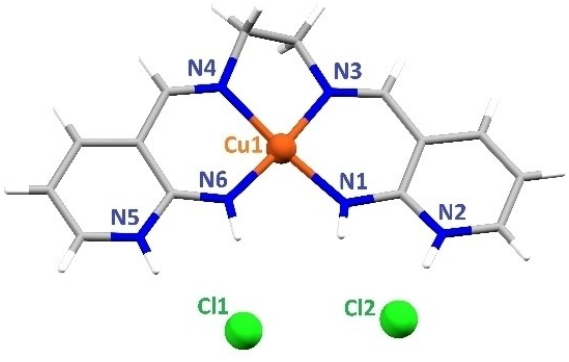

Figure 1. Representation of the crystal structure of **1**. The atoms bonded to the metal centre and the chloride anions are labelled.

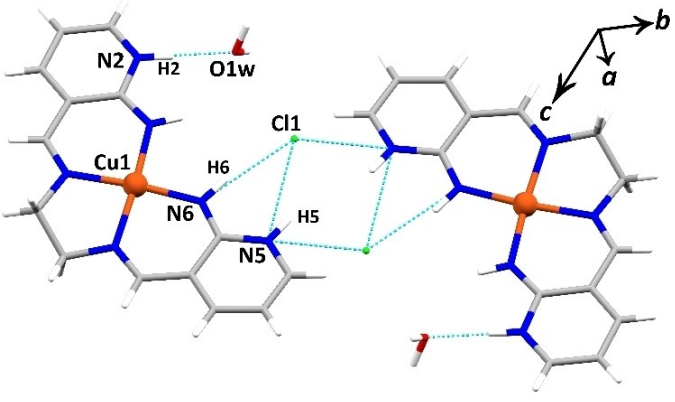

Figure 2. Representation of a dimer of [Cu(**en2ampy**)]$^{2+}$ cations connected through hydrogen bonding with two chloride anions.

Research Article
doi.org/10.1002/ejic.202400159

formed of "cyclohexyl-type" motifs in chair conformation, made of four water molecules and two opposite chlorides (see Figure S3 top). These "cyclohexyl-type" unit are connected via two chlorides and two water molecules to generate the supramolecular chain along the crystallographic *a* axis (Figure S3 bottom). These chains are hydrogen bonded to the $[Cu(\mathbf{en2ampy})]^{2+}$ stacks by means of hydrogen bonds involving the pyridinium nitrogen N6, water molecule O1w and chloride anion Cl2.

Complex **2** crystallizes in the monoclinic space group $P2_1/n$ (Table S1). A representation of its solid-state structure is shown in Figure 3.

The structure of the cationic $[Cu(\mathbf{en2ampy})]^{2+}$ unit is similar to that observed in **1** (see above). The square-planar copper(II) center exhibits coordination angles varying from 83.69(5) to 93.55(5) (Table S2). The N(imine)-Cu bond distances (N3 and N4) are 1.961(1) and 1.963(1) Å. As observed for **1**, the N(anilido)-Cu bond lengths are shorter, *viz.* 1.933(1) Å for N1 and 1.925(1) Å for N6 (Table S2).

The crystal lattice of **2** does not contain water molecules; hence, the packing of the molecules is simpler than that of **1**. The $[Cu(\mathbf{en2ampy})]^{2+}$ cations form dimers through hydrogen bonding between two nitrate anions (N7), one of the pyridinium units (N2) and an anilido moiety (N6) (Table S3), as depicted in Figure S4. Moreover, stacks between two $[Cu(\mathbf{en2ampy})]^{2+}$ units are observed, which are separated by a distance of 3.527(1) Å (*Cg*4···*Cg*5; Figure S5). These dimers interact with other such stacks π–π contacts, symbolized by a centroid-to-centroid distance of 3.527(1) Å; this supramolecular assembly generates voids where are located the nitrate anions (Figure S5).

DNA Interaction

The potential interaction of **1** and **2** with DNA was examined using different techniques.

UV-Vis spectroscopy: increasing concentrations of *Calf Thymus* DNA (ct-DNA), *i.e.* 0–100 μM, were added to 25 μM solutions of **1** and **2** (see Experimental Section for details). The corresponding UV-Vis spectra for **1** (recorded in the range 500–200 nm) are shown in Figure 4. Upon increasing the concentration of DNA, a slight decrease in the intensity of the three absorption bands is observed; moreover, a small red shift (from 381 to 387 nm) is noted when more than 1 equivalent of DNA is added to the complex solution. This hypochromic effect and subsequent red shift of the absorption bands may be attributed to the intercalation of **1** between DNA base pairs.[23] The corresponding binding constant K_b was determined (see Experimental Section for details and Figure S6), and estimated to be of $3.59 \pm 0.29 \times 10^5$ M^{-1}. The DNA-binding affinity of **1** is lower than that of the classical intercalator ethidium bromide, which has K_b values of 7×10^7 M^{-1} in 40 mM Tris-HCl buffer, pH 7.9,[24] and 1.4×10^6 M^{-1} in 40 mM NaCl-25 mM Tris-HCl.[25]

Unsurprisingly, comparable features were obtained for complex **2** (Figure S7). A binding constant K_b of $3.37 \pm 0.28 \times 10^5$ M^{-1} could be determined (Figure S8).

Fluorescence spectroscopy: Competitive binding studies with the DNA intercalator ethidium bromide (EB) were then carried out using fluorescence spectroscopy. The fluorescence of EB increases when the EB-DNA adduct is formed; hence, its displacement by an intercalative molecule will lead to a decrease of the fluorescence.[26]

As evidenced in Figure 5, increasing addition of **1** ([complex] = 0–200 μM) to the EB-DNA adduct ([EB-DNA] = 25 μM) leads to a decrease in fluorescence, thus suggesting that the planar copper complex (Figure S1) can replace EB between DNA base pairs. Though, it can be pointed out here that such EB displacement by the cationic $[Cu(\mathbf{en2ampy})]^{2+}$ species may not necessarily arise from its intercalation; indeed, significant electrostatic or groove-binding interactions may modify the DNA double helix resulting in EB displacement. One may consider that the $[Cu(\mathbf{en2ampy})]^{2+}$ cations may electrostatically

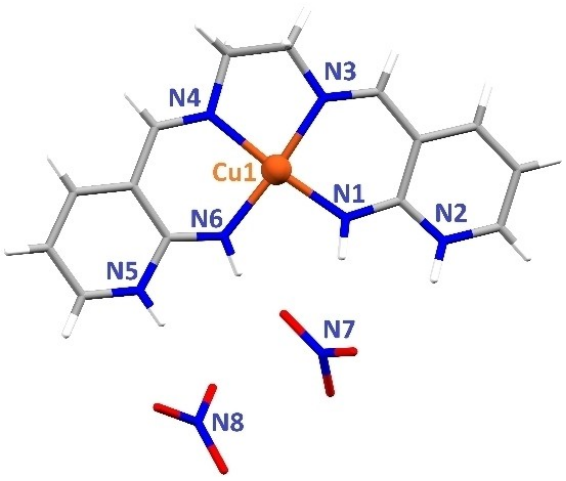

Figure 3. Representation of the crystal structure of **2**. The atoms bonded to the metal centre and the nitrate anions are labelled.

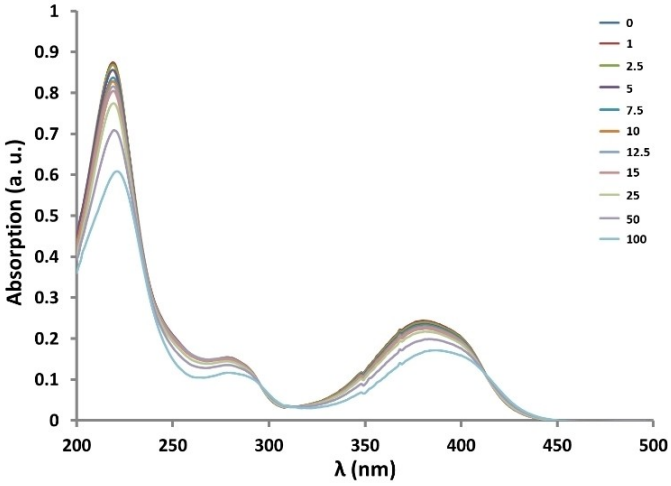

Figure 4. UV-Vis spectra of 25 μM solutions of **1** in the absence and presence of increasing amounts of ct-DNA (0–100 μM). The DNA-binding studies were carried out in cacodylate–NaCl buffer at 37 °C. The spectra were recorded after an incubation time of 24 h.

Research Article
doi.org/10.1002/ejic.202400159

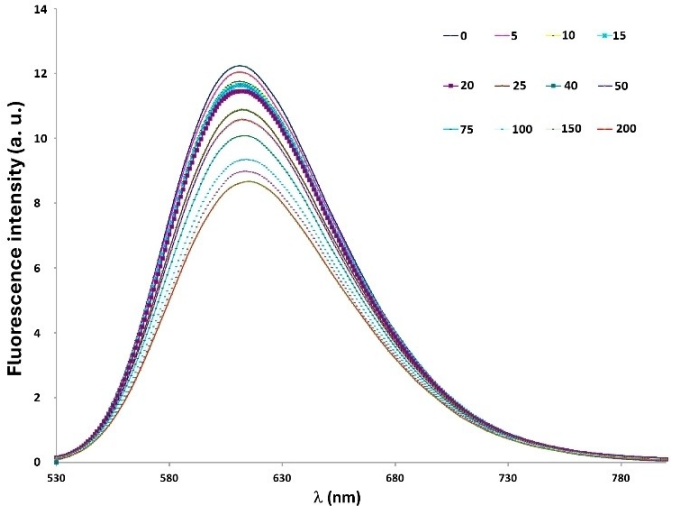

Figure 5. Competitive displacement assays for DNA-EB adducts upon addition of increasing amounts of **1**. Experimental data points obtained after 1 h of incubation and using [DNA] = 25 μM_{bp}, [EB] = 25 μM and [complex] = 0–200 μM. λ_{exc} = 514 nm; λ_{em} = 610 nm.

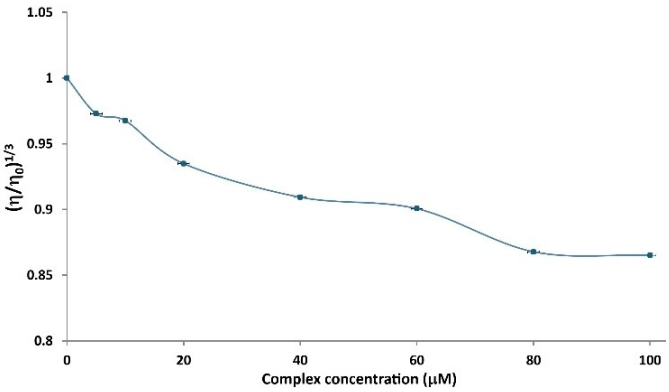

Figure 6. Plot of relative viscosity (η/η_0) *versus* the concentration of complex **1**. [DNA] = 150 μM; [**1**] = 0–100 μM. Measurements carried out in TE buffer (pH 7.4) at 20 °C. Data points obtained after 1 h incubation after the addition of the complex.

interact with the negative phosphate backbone of the double helix. The "strength" of this interaction was estimated by calculating the corresponding Stern-Volmer K_{sv} constant by using the I_0/I *vs.* [complex] plot shown in Figure S9 (see Experimental Section for details). The low K_{sv} value of $3.3 \pm 0.4 \times 10^3$ M^{-1} ($< 10^4$ M^{-1})[27] obtained indicates that **1** does not act as an intercalator; it most likely interacts electrostatically with the biomolecule, possibly as groove binder.[28] Unsurprisingly, complex **2** exhibits comparable features, with a K_{sv} value of $3.9 \pm 0.9 \times 10^3$ M^{-1} (Figures S10 and S11).

Viscosity: The nature of the interaction between a molecule and DNA can be investigated by changes of the viscosity of solutions of the double helix.[29] Intercalative compounds typically give rise to a lengthening of the DNA helix as the result of the separation of base pairs, which increases the DNA-solution viscosity.[30] In contrast, groove binders induce a twisting and shortening of the helix, hence decreasing the viscosity of the DNA solution.[31]

The effect of **1** on the viscosity of a 150 μM solution of ct-DNA in TE buffer (pH 7.4) was investigated at 20 °C. Upon increasing the concentration of **1** (from 0 to 100 μM), a slight decrease of the viscosity of the DNA solution was observed (Figure 6).

The data achieved confirm that **1** is not a DNA intercalator since a decrease in viscosity was observed, suggesting that the "external" (*viz.*, non-intercalative) interaction of **1** with DNA induces a static bend or kink in the double helix.[32] As expected, a comparable behaviour was found for complex **2** (Figure S12).

Electrophoresis: The interaction of complexes **1** and **2** with plasmid pBR322 DNA was investigated by agarose gel electrophoresis. The study was carried out in the presence or not of ascorbic acid, which mimics the reducing environment found inside cells. Furthermore, the complex $[Cu(Phen)_2(H_2O)](NO_3)_2$ (Phen = 1,10-phenanthroline) also known as Sigman's complex,[33] was used as reference complex. The gel image for **1** is shown in Figure 7.

Free DNA shows the supercoiled (Form I) and circular nicked forms (Form II) (Lanes 1 and 9). In the presence of ascorbic acid, Form I almost disappears and is converted into Form II (Lanes 10 and 13). With the reference Sigman's complex, DNA cleavage is clearly observed (Lanes 11 and 12, especially in the presence of the reducing agent (see Lane 12; the DNA is completely degraded). Comparatively, complex **1** does not significantly affect the biomolecule (Lanes 2–8 and Lanes 14–19). Some increase of Form II is observed in the absence of reducing agent from a [complex **1**] ≥ 80 μM (Lanes 7 and 8). In the presence of ascorbic acid, such an increase of Form II is observed from a complex concentration of 5 μM (Lanes 14–19). The electrophoresis data suggest that complex **1** does not act as an artificial nuclease, in contrast to $[Cu(Phen)_2(H_2O)](NO_3)_2$. Most likely, the non-intercalative interaction of **1** with DNA produces some Form II (a redox pathway does not appear to take place; at least, that does not seem to be a dominant pathway). As evidenced in Figure S13, an analogous behaviour is found for complex **2**.

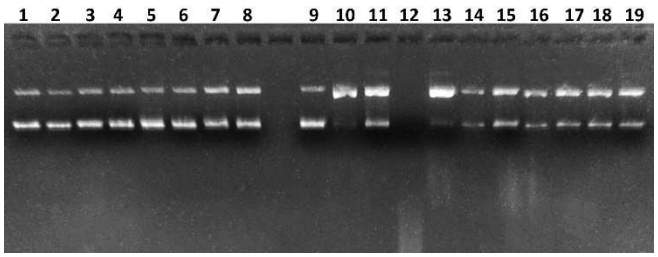

Figure 7. Agarose gel electrophoresis image of 15 μM_{bp} pBR322 plasmid DNA incubated for 1 h at 37 °C with increasing concentrations of complex **1**, without and with ascorbic acid (as reducing agent). The reference complex $[Cu(Phen)_2(H_2O)](NO_3)_2$ was used for comparison purposes. Lanes 1 and 9: plasmid DNA; Lanes 2–8: DNA + **1** (5, 10, 20, 40, 60, 80 and 100 μM); Lanes 10 and 13: DNA + ascorbic acid (1 mM); Lane 11: DNA + $[Cu(Phen)_2(H_2O)](NO_3)_2$ (5 μM); Lane 12: DNA + $[Cu(Phen)_2(H_2O)](NO_3)_2$ (5 μM) + ascorbic acid (1 mM); Lanes 14–19: DNA + **1** (5, 10, 20, 40, 60, 80 and 100 μM) + ascorbic acid (1 mM).

Research Article
doi.org/10.1002/ejic.202400159

Cytotoxicity

The potential cytotoxic properties of complexes **1** and **2** were evaluated against human ovarian carcinoma (A2780) cells and their cisplatin resistant (A2780Cis) line. Half-maximum inhibitory concentrations (IC_{50}) were determined for the two compounds after incubation times of 24 and 72 h (Figure S14). The IC_{50} values obtained are listed in Table 1 and are compared with those of cisplatin. Although the two complexes do not seem to function as chemical nucleases, **1** and **2** show significant cytotoxic properties, with IC_{50} values ranging from 2.06 to 9.82 μM (Table 1). After 72 h of incubation, the compounds are especially efficient with IC_{50}'s of 3.01 ± 0.44 and 2.06 ± 0.54 μM for **1** and **2**, respectively. Interestingly, these compounds are 7 to 10 times more active than cisplatin against resistant A2780Cis cells after 24 h of incubation and are still twice more active than cisplatin after 72 h of incubation (Table 1). Although, the DNA interaction of these copper compounds appears to be distinct to that of cisplatin, they are somehow affected by the resistance mechanism(s) of A2780Cis cells as they are slightly less efficient compared to their respective activities against A2780 cells. From the electrophoretic studies, it seems that the planar dicationic [Cu(**en2ampy**)]$^{2+}$ species is capable of inducing cell death without the involvement of radical species (generated through a redox process). Indeed, the complex-mediated generation of radicals would have produced DNA form III in the electrophoresis gels (see **Electrophoresis** section; Figure 7). In contrast to the well-known cytotoxic, DNA cleaver $[Cu(Phen)_2(H_2O)](NO_3)_2$, **1** and **2** do not induce a strong DNA degradation, hence indicating that their mechanism of action is probably different from that of Sigman's complex.

Conclusions

The use of a simple tetradentate Schiff-base ligand with two different copper(II) salts produced two square-planar complexes that exhibit an uncommon feature; indeed, the ligand acts as an N_2/N_2^{2-}-donor moiety. Thus, two aromatic $-NH_2$ groups are deprotonated and are coordinated as very rare $-NH^-$ (amido) donors to the copper centre. This amine deprotonation is most likely facilitated by the neighbouring pyridine units of the ligand **en2ampy**, which therefore has a zwitterionic character. Although it is highly planar, the doubly charged complex cation [Cu(**en2ampy**)]$^{2+}$ is not intercalating between DNA base pairs; instead, it appears to interact electrostatically with the double helix, probably in the grooves. Moreover, the copper(II) complexes are not efficient DNA cleavers (even in the presence of a reducing agent); nevertheless, they show interesting cytotoxic properties, with IC_{50} values down to 2 μM. Remarkably, these copper compounds are more cytotoxic than cisplatin in the two cell lines tested; for instance, it can be stressed that they are 2.5–3.2 more active than cisplatin against the ovarian cell line A2780 and, more importantly, 7.6–10.7 more active than cisplatin against cisplatin-resistant A2780Cis cells after 24 h of incubation. Since the simple **en2ampy** ligand (obtained in a one-step reaction) allowed to generate a [Cu(**en2ampy**)]$^{2+}$ species with attractive cytotoxic properties, new members of this new family of ligand will be prepared, for instance using other (bridging) diamines. The use of functionalized 2-amino-nicotinaldehydes may also be envisaged.

Experimental Section

Materials and methods: The solvents, reagents to prepare the ligand and for the spectroscopic studies were obtained from commercial sources and used as received. pBR322 plasmid DNA and *Calf-Thymus* DNA (ct-DNA) were purchased from ThermoFisher Scientific. SYBR safe and 10× TBE buffer were obtained from Invitrogen. Agarose was purchased from Ecogen. ^1H and $^{13}C\{^1H\}$ NMR spectra were recorded at room temperature with 300 or 400 MHz spectrometers. Chemical shifts are reported downfield from standards and the coupling constants are given in Hz. All NMR data were analyzed using MestRe Nova Version 14.2.1.[36] The IR spectra were recorded using Attenuated Total Reflection (ATR) with a Nicolet-5700 FT-IR (in the range 4000–400 cm^{-1}) and the main absorption bands are expressed in cm^{-1}. Elemental analyses were performed by the Servei de Microanalisi, Serveis Cientificotècnics of the University of Barcelona. UV/Vis spectra were recorded with a Varian Cary 100 scan spectrometer with a 1 cm path length quartz cuvette. Fluorescence studies were carried out on a HORIBA Jobin-Yvon iHR320 fluorometer with a 1 cm path-length quartz cuvette. Viscosity measurements were performed with an AND-SV-1 viscometer in a water bath using a water jacket accessory and maintained at a constant temperature of 25 °C.

Preparation of the ligand en2ampy, namely 3,3′-((1*E*,1′*E*)-(ethane-1,2-diylbis(azaneylylidene))bis(methaneylylidene))bis(pyridin-2-amine): 0.09 g (1.5 mmol) of ethylenediamine and 0.368 g (3.0 mmol) of 2-aminonicotinaldehyde were dissolved in 20 mL of ethanol. After a few minutes, the clear solution was refluxed for 3 h. The resulting white precipitate was isolated by filtration and

Table 1. IC_{50} values[a] (μM) of compounds **1**, **2** and cisplatin in A2780 (human ovarian carcinoma) and A2780Cis (human ovarian carcinoma resistant to cisplatin) cells.

	24 h		72 h	
Compound	IC_{50} (μM) A2780	IC_{50} (μM) A2780Cis	IC_{50} (μM) A2780	IC_{50} (μM) A2780Cis
1	6.66 ± 0.23	9.82 ± 0.28	3.01 ± 0.44	6.44 ± 0.23
2	5.08 ± 0.23	7.02 ± 0.49	2.06 ± 0.54	5.69 ± 0.10
Cisplatin	16.41[34]	74.97[34]	2.8 ± 0.20[35]	13.8 ± 0.20[35]

[a] The results are expressed as mean values ± SD out of three independent experiments.

Research Article
doi.org/10.1002/ejic.202400159

washed with 3×10 mL of ethanol. After drying in air, 0.279 g of pure **en2ampy** were obtained.

$C_{14}H_{16}N_6$; $M_w = 268.32\ g\,mol^{-1}$. Yield = 69%. CHN calcd. (found) in %: C 62.67 (62.22), H 6.01 (5.96), N 31.32 (31.28). ^1H NMR ($CDCl_3$): $\delta =$ 8.26 (s, 2 H), 8.06 (d, $J = 6.8$ Hz, 2H), 7.45 (d, $J = 7.2$ Hz, 2 H), 6.62 (dd, $J = 7.6$ Hz, $J = 7.6$ Hz, 2 H), 3.93 (s, 4 H) (Figure S15). ^{13}C NMR ($CDCl_3$): $\delta = 163.9$, 159.2, 150.1, 141.3, 112.6, 62.6 (Figure S16). IR (ATR measurement, 32 scans, cm^{-1}): $\tilde{\nu} = 3304$, 3122, 2904, 2843, 1639, 1565 (Figure S17).

Preparation of the complex [Cu(en2ampy)]$Cl_2(H_2O)_2$ (1): 68.2 mg (0.4 mmol) of $CuCl_2 \cdot 2H_2O$ were dissolved in 30 mL of ethanol. Subsequently, a solution of 175.5 mg (0.4 mmol) of **en2ampy** in 10 mL of ethanol was added dropwise. The resulting reaction mixture was stirred for 1 h at room temperature. Then, the brown precipitate formed was isolated by filtration and washed with 10 mL of ethanol. After drying in air, 0.134 g of complex **1** was obtained as a yellow powder. Single crystals of **1**, suitable for X-ray diffraction analysis could be obtained from diffusion of diethyl ether (2 mL) into a methanolic solution (2 mL; 0.1 mM) of the complex in a closed system (namely the complex solution was added to a 5 mL flask, which was introduced in a 20 mL flask containing diethyl ether). Complex **1** is soluble in water and methanol. $C_{14}H_{20}Cl_2CuN_6O_2$; $M_w = 438.80\ g\,mol^{-1}$. Yield = 77%. CHN calcd. (found) in % (for **1**): C 38.64 (38.32), H 4.37 (4.59), N 19.24 (19.15). IR (ATR measurement, 32 scans, cm^{-1}): $\tilde{\nu} = 3407$, 3134, 1657, 1596, 1474, 1230, 713 (Figure S18).

Preparation of the complex [Cu(en2ampy)]$(NO_3)_2$ (2): 186 mg (0.4 mmol) of $Cu(NO_3)_2 \cdot 2.5H_2O$ were dissolved in 30 mL of ethanol. Next, a solution of 175.5 mg (0.4 mmol) of **en2ampy** in 10 mL of ethanol was added dropwise. The ensuing reaction mixture was stirred for 1 h at room temperature. The resulting brown precipitate was isolated by filtration and washed with 10 mL of ethanol. After drying in air, 0.153 g of complex **2** was obtained as a light-orange powder. Single crystals, suitable for X-ray diffraction analysis were obtained from diffusion of diethyl ether into a methanolic solution of the complex, using the same procedure as that applied for **1**. Complex **2** is soluble in water and methanol. $C_{14}H_{16}CuN_8O_6$; $M_w = 455.88\ g\,mol^{-1}$. Yield = 84%. CHN calcd. (found) in % (for $\mathbf{2} \cdot H_2O$): C 35.56 (35.48), H 3.62 (3.83), N 23.70 (23.65). IR (ATR measurement, 32 scans, cm^{-1}): $\tilde{\nu} = 3409$, 3339, 3248, 3143, 3070, 1657, 1596, 1478, 1383, 1234, 1113, 800, 752 (Figure S19).

X-ray crystallography: Data for compounds **1** and **2** were obtained at 100 K respectively on a 0.12×0.02×0.01 mm^3 yellow lath and a 0.11×0.08×0.06 mm^3 cubic block at Beamline 11.3.1 of the Advanced Light Source (Berkeley, USA), on a Bruker D8 diffractometer equipped with a PHOTON 100 detector and using silicon (111) monochromated synchrotron radiation ($\lambda = 0.7749$ Å). Data reduction and absorption corrections were performed with SAINT and SADABS, respectively.[37] The structures were solved by intrinsic phasing with SHELXT,[38] and refined by full-matrix least-squares on F^2 with SHELXL.[39] All details can be found in CCDC 2339037 (**1**) and 2339038 (**2**) that contain the supplementary crystallographic data for this paper. These data can be obtained free of charge from The Cambridge Crystallographic Data Center via https://www.ccdc.cam.ac.uk/structures/. Crystallographic and refinement parameters are summarized in Table S1. Details of hydrogen bonds involving the guest anions and of the coordination environment of the Cu(II) ions are given in Tables S2 and S3 respectively.

UV-Vis spectroscopy: Stock solutions (1 mL) of complexes **1** and **2** (5 mM) were prepared in milli-Q water, just before use. The samples to be analysed were prepared by the addition of increasing amounts of ct-DNA (from 0 to 100 μM, in base pairs) to a 25 μM solution of the complex tested. The UV-Vis spectra were recorded using a Varian Cary-100 spectrophotometer.

Fluorescence spectroscopy: Stock solutions (1 mL) of the two complexes (5 mM) were prepared in milli-Q water. The samples to be analyzed were prepared by addition of aliquots of the freshly prepared stock solutions of the complex (in the concentration range 0–200 μM.) to the appropriate volume of ct-DNA in 1 mM sodium cacodylate–20 mM NaCl buffer (pH = 7.2). A solution ct-DNA/EB (*i.e.*, without complex) in cacodylate buffer was used as a blank sample. Fluorescence spectra were recorded at constant concentrations of EB and ct-DNA, *viz.*, 25 μM at room temperature, after 24 h incubation at 37 °C, on a Nandog™-Horiba Jobin Yvon spectrofluorometer with a 450 W xenon lamp using a computer for spectral subtraction and noise reduction. Each sample was scanned twice in a range of wavelengths between 500 and 800 nm, after excitation at 520 nm.

Viscosity measurements: Viscosity experiments were performed with an AND-SV-1 viscometer in a water bath at a constant temperature of 25 °C using a water jacket accessory. The hydrophilic compounds were dissolved in milli-Q water. The samples were prepared by addition of aliquots of the stock aqueous solutions of the complexes to the appropriate volume of ct-DNA in a TE buffer (50 mM NaCl, 10 mM tris-(hydroxymethyl)aminomethane hydrochloride (Tris–HCl), 0.1 mM H4edta, pH 7.4) (5 mL). A solution of free native DNA in TE was used as a blank sample. The viscosity spectra of DNA in the presence or absence of the complexes ([ct-DNA] = 25 μM; [complex] = 0–200 μM) were recorded at 25 °C, after incubation of 1 h at 37 °C.

Gel electrophoresis: Stock solutions of **1** and **2** were prepared in 1 mM sodium cacodylate–20 mM NaCl buffer (pH = 7.2). pBR322 plasmid DNA aliquots (25 μM in base pairs) in 1 mM cacodylate–20 mM NaCl buffer were incubated with the complexes (0–100 μM) for 1 h at 37 °C. For the studies with the reducing agent, namely ascorbic acid (1 mM in cacodylate–20 mM NaCl buffer), it was subsequently added and the resulting mixture was incubated at 37 °C for an additional hour. The reaction samples were then quenched with 4 μL of a xylene cyanol 1X aqueous solution (containing 30% (v/v) glycerol, 0.25% (w/v) bromophenol blue and 0.25% (w/v) xylene cyanol), and consequently electrophoretized in agarose gel (1% in TAE buffer) for 1 h at 1.5 $V\,cm^{-1}$, using a Bio-Rad horizontal tank connected to a Consort EV231 variable potential power supply. The DNA was subsequently stained with SYBR® safe and the gel was photographed with a BIORAD Gel Doc™ EZ Imager. Samples containing free DNA and DNA with ascorbic acid were used as controls.

Cytotoxicity studies: Human ovarian carcinoma cell line A2780 (ECACC 93112519) and its derived cisplatin resistant cell line A2780 cis (ECACC 93112517) were routinely maintained in RPMI 1640 medium (Gibco) supplemented with 10% heat-inactivated Foetal Bovine Serum (FBS), GlutaMAX™ (Gibco) and 1% Antibiotic-Antimycotic (Gibco), in standard growth conditions (37 °C and 5% CO2). All tested compounds were kept in DMSO stocks at 50 mM and stored at −20 °C. All working concentrations were prepared in cell culture media with a maximum of 0.5% of DMSO. Cells of each cell line in exponential growth were seeded into 96-well plates at a density of 3×10^3 cells/well and were allowed to grow overnight. After that, cells were treated with different concentrations of each compound, ranging from 100 nM to 200 μM, during 24 h and 72 h and then 10 μL of PrestoBlue reagent (Invitrogen) were added following the standard protocol (Xu et al., 2015). After 3 h incubation, fluorescence was measured exciting at 531 nm (emission at 572 nm) using a Victor3 multiwell microplate reader (Perkin Elmer). The relative cell viability (%) for each sample related to the

control cells without treatment was calculated. Each sample was tested in triplicates, in three independent experiments.

Supporting Information

X-ray data (Tables S1, S2 and S3); representation of zwitterionic **en2ampy** (Scheme S1); representation of the planar [Cu(**en2ampy**)]$^{2+}$ unit (Figure S1); representations of the crystal packing of **1** and **2** (Figures S2–S5); [DNA]/(ε_a-ε_f) *vs.* [DNA] plot for **1** (Figure S6); UV-Vis spectra of **2** (Figure S7); [DNA]/(ε_a-ε_f) *vs.* [DNA] plot for **2** (Figure S8); Stern-Volmer plots for **1** (Figure S9); Competitive displacement assays for DNA-EB adducts for **2** (Figure S10); Stern-Volmer plots for **2** (Figure S11); Plot of relative viscosity for **2** (Figure S12); gel electrophoresis image for **2** (Figure S13); Percent cell viability *versus* complex concentration for **1** and **2** (Figure S14); IR and NMR spectra of **en2ampy** (Figures S15–S17); IR spectra of **1** and **2** (Figures S18 and S19.

Acknowledgements

Financial support from the Spanish Ministerio de Ciencia e Innovación (Projects PID2020-115537RB-I00 and PCI2021-122027-2B, MCIN/AEI /10.13039/501100011033 and "European Union NextGenerationEU/PRTR) is kindly acknowledged.

Conflict of Interests

The authors declare no conflict of interest.

Data Availability Statement

The data that support the findings of this study are available from the corresponding author upon reasonable request.

Keywords: Copper · Square-Planar Ligand · Amido Ligands · DNA Interaction · Cytotoxicity

[1] a) H. Sung, J. Ferlay, R. L. Siegel, M. Laversanne, I. Soerjomataram, A. Jemal, F. Bray, *Ca-Cancer J. Clin.* **2021**, *71*, 209–249; b) R. L. Siegel, K. D. Miller, N. S. Wagle, A. Jemal, *Ca-Cancer J. Clin.* **2023**, *73*, 17–48.
[2] World Health Organization, **2024**, https://www.who.int/news/item/01-02-2024-global-cancer-burden-growing-amidst-mounting-need-for-services, March 6th 2024.
[3] S. Sen, M. Won, M. S. Levine, Y. Noh, A. C. Sedgwick, J. S. Kim, J. L. Sessler, J. F. Arambula, *Chem. Soc. Rev.* **2022**, *51*, 1212–1233.
[4] a) C. Sonkar, S. Sarkar, S. Mukhopadhyay, *RSC Med. Chem.* **2022**, *13*, 22–38; b) S. Abdolmaleki, A. Aliabadi, S. Khaksar, *Coord. Chem. Rev.* **2024**, *501*, 32; c) G. Moreno-Alcántar, P. Picchetti, A. Casini, *Angew. Chem. Int. Ed.* **2023**, *62*, 32.
[5] a) R. A. Alderden, M. D. Hall, T. W. Hambley, *J. Chem. Educ.* **2006**, *83*, 728–734; b) S. Gómez-Ruiz, D. Maksimovic-Ivanic, S. Mijatovic, G. N. Kaluderovic, *Bioinorg. Chem. Appl.* **2012**, *2012*, 14.
[6] H. Tapiero, D. M. Townsend, K. D. Tew, *Biomed. Pharmacother.* **2003**, *57*, 386–398.
[7] a) F. P. E. Vairo, B. C. Chwal, S. Perini, M. A. P. Ferreira, A. C. F. Lopes, J. A. M. Saute, *Mol. Genet. Metab.* **2019**, *126*, 6–13; b) A. Czlonkowska, T. Litwin, P. Dusek, P. Ferenci, S. Lutsenko, V. Medici, J. K. Rybakowski, K. H. Weiss, M. L. Schilsky, *Nat. Rev. Dis. Primers* **2018**, *4*, 20.
[8] a) J. J. Wilson, S. J. Lippard, *Chem. Rev.* **2014**, *114*, 4470–4495; b) S. Thota, D. A. Rodrigues, D. C. Crans, E. J. Barreiro, *J. Med. Chem.* **2018**, *61*, 5805–5821; c) S. A. Sharma, P. Sudhindra, N. Roy, P. Paira, *Inorg. Chim. Acta* **2020**, *513*, 18; d) C. C. Konkankit, S. C. Marker, K. M. Knopf, J. J. Wilson, *Dalton Trans.* **2018**, *47*, 9934–9974; e) A. R. Kapdi, I. J. S. Fairlamb, *Chem. Soc. Rev.* **2014**, *43*, 4751–4777.
[9] a) C. Santini, M. Pellei, V. Gandin, M. Porchia, F. Tisato, C. Marzano, *Chem. Rev.* **2014**, *114*, 815–862; b) C. H. Wang, X. D. Yang, C. Y. Dong, K. K. Chai, J. Ruan, S. Shi, *Coord. Chem. Rev.* **2023**, *487*, 30.
[10] L. A. Alfonso-Herrera, S. Rosete-Luna, D. Hernández-Romero, J. M. Rivera-Villanueva, J. L. Olivares-Romero, J. A. Cruz-Navarro, A. Soto-Contreras, A. Arenaza-Corona, D. Morales-Morales, R. Colorado-Peralta, *ChemMedChem* **2022**, *17*, 42.
[11] a) L. M. Balsa, M. R. Rodriguez, B. S. Parajón-Costa, A. C. González-Baró, M. J. Lavecchia, I. E. León, *ChemMedChem* **2022**, *17*, 13; b) R. K. Lin, C. I. Chiu, C. H. Hsu, Y. J. Lai, P. Venkatesan, P. H. Huang, P. S. Lai, C. C. Lin, *Chem. Eur. J.* **2018**, *24*, 4111–4120; c) I. Besleaga, I. Stepanenko, T. V. Petrasheuskaya, D. Darvasiova, M. Breza, M. Hammerstad, M. A. Marc, A. Prado-Roller, G. Spengler, A. Popovic-Bijelic, E. A. Enyedy, P. Rapta, A. D. Shutalev, V. B. Arion, *Inorg. Chem.* **2021**, *60*, 11297–11319.
[12] K. Muñiz, *Angew. Chem. Int. Ed.* **2005**, *44*, 6622–6627.
[13] X. F. Wu, C. Wang, J. L. Xiao, *Platinum Met. Rev.* **2010**, *54*, 3–19.
[14] M. W. Johnson, A. G. DiPasquale, R. G. Bergman, F. D. Toste, *Organometallics* **2014**, *33*, 4169–4172.
[15] C. Tejel, M. A. Ciriano, M. P. del Río, D. G. H. Hetterscheid, N. T. I. Spithas, J. M. M. Smits, B. de Bruin, *Chem. Eur. J.* **2008**, *14*, 10932–10936.
[16] C. Tejel, M. P. del Río, L. Asensio, F. J. van den Bruele, M. A. Ciriano, N. T. I. Spithas, D. G. H. Hetterscheid, B. de Bruin, *Inorg. Chem.* **2011**, *50*, 7524–7534.
[17] a) I. C. Cai, M. I. Lipschutz, T. D. Tilley, *Chem. Commun.* **2014**, *50*, 13062–13065; b) R. Weller, M. Atanasov, S. Demeshko, T. Y. Chen, I. Mohelsky, E. Bill, M. Orlita, F. Meyer, F. Neese, C. G. Werncke, *Inorg. Chem.* **2023**, *62*, 3153–3161; c) A. J. C. De Lucio, I. C. Cai, R. J. Witzke, A. N. Desnoyer, T. D. Tilley, *Organometallics* **2022**, *41*, 1434–1444; d) R. Weller, L. Völlinger, C. G. Werncke, *Eur. J. Inorg. Chem.* **2021**, *2021*, 4383–4392; e) L. J. Taylor, D. L. Kays, *Dalton Trans.* **2019**, *48*, 12365–12381.
[18] C. L. Wagner, L. Z. Tao, E. J. Thompson, T. A. Stich, J. D. Guo, J. C. Fettinger, L. A. Berben, R. D. Britt, S. Nagase, P. P. Power, *Angew. Chem. Int. Ed.* **2016**, *55*, 10444–10447.
[19] N. P. Mankad, W. E. Antholine, R. K. Szilagyi, J. C. Peters, *J. Am. Chem. Soc.* **2009**, *131*, 3878–3880.
[20] a) S. Wiese, Y. M. Badiei, R. T. Gephart, S. Mossin, M. S. Varonka, M. M. Melzer, K. Meyer, T. R. Cundari, T. H. Warren, *Angew. Chem. Int. Ed.* **2010**, *49*, 8850–8855; b) M. M. Melzer, S. Mossin, X. Dai, A. M. Bartell, P. Kapoor, K. Meyer, T. H. Warren, *Angew. Chem. Int. Ed.* **2010**, *49*, 904–907.
[21] L. A. Goj, E. D. Blue, C. Munro-Leighton, T. B. Gunnoe, J. L. Petersen, *Inorg. Chem.* **2005**, *44*, 8647–8649.
[22] a) M. McCann, J. F. Cronin, M. Devereux, V. McKee, G. Ferguson, *Polyhedron* **1995**, *14*, 3617–3626; b) A. Grirrane, E. Alvarez, H. García, A. Corma, *Angew. Chem. Int. Ed.* **2014**, *53*, 7253–7258.
[23] a) A. M. Pyle, J. P. Rehmann, R. Meshoyrer, C. V. Kumar, N. J. Turro, J. K. Barton, *J. Am. Chem. Soc.* **1989**, *111*, 3051–3058; b) N. Kumar, R. Kaushal, P. Awasthi, *J. Mol. Struct.* **2023**, *1288*, 135751.
[24] M. J. Waring, *J. Mol. Biol.* **1965**, *13*, 269–282.
[25] J. B. Lepecq, C. Paoletti, *J. Mol. Biol.* **1967**, *27*, 87–106.
[26] S. R. Gallagher, P. R. Desjardins, *Current protocols in molecular biology* **2006**, *Appendix 3*, Appendix 3D.
[27] K. Ypsilantis, E. Sifnaiou, A. Garypidou, D. Kordias, A. Magklara, A. Garoufis, *Molecules* **2024**, *29*, 514–529.
[28] C. P. Popolin, J. P. B. Reis, A. B. Becceneri, A. E. Graminha, M. A. P. Almeida, R. S. Corrêa, L. A. Colina-Vegas, J. Ellena, A. A. Batista, M. R. Cominetti, *PLoS One* **2017**, *12*, e0183275.
[29] a) L. S. Lerman, *J. Mol. Biol.* **1961**, *3*, 18–30; b) N. Varghese, J. R. Jose, P. M. Krishna, D. Philip, F. Joy, T. P. Vinod, M. R. P. Kurup, Y. Nair, *ChemistrySelect* **2023**, *8*, e202203615.
[30] S. Satyanarayana, J. C. Dabrowiak, J. B. Chaires, *Biochemistry* **1993**, *32*, 2573–2584.
[31] J. M. Kelly, A. B. Tossi, D. J. McConnell, C. Ohuigin, *Nucleic Acids Res.* **1985**, *13*, 6017–6034.
[32] a) J. P. Quinn, D. J. McGeoch, *Nucleic Acids Res.* **1985**, *13*, 8143–8163; b) R. Gup, C. Gökçe, N. Dilek, *J. Photochem. Photobiol. B* **2015**, *144*, 42–50; c) P. R. Reddy, A. Shilpa, *Chem. Biodiversity* **2011**, *8*, 1245–1265.

Research Article
doi.org/10.1002/ejic.202400159

[33] K. A. Reich, L. E. Marshall, D. R. Graham, D. S. Sigman, *J. Am. Chem. Soc.* **1981**, *103*, 3582–3584.
[34] M. L. Krieger, N. Eckstein, V. Schneider, M. Koch, H. D. Royer, U. Jaehde, G. Bendas, *Int. J. Pharm.* **2010**, *389*, 10–17.
[35] R. Raveendran, J. P. Braude, E. Wexselblatt, V. Novohradsky, O. Stuchlikova, V. Brabec, V. Gandin, D. Gibson, *Chem. Sci.* **2016**, *7*, 2381–2391.
[36] M. R. Willcott, *J. Am. Chem. Soc.* **2009**, *131*, 13180–13180.
[37] G. M. Sheldrick, *SAINT and SADABS*, Bruker AXS Inc., Madison, Wisconsin, USA, **2012**.
[38] G. M. Sheldrick, *Acta Crystallogr. Sect. A* **2015**, *71*, 3–8.
[39] G. M. Sheldrick, *Acta Crystallogr. Sect. C-Struct. Chem.* **2015**, *71*, 3–8.

Manuscript received: March 20, 2024
Revised manuscript received: April 26, 2024
Accepted manuscript online: May 20, 2024
Version of record online: ■■, ■■

RESEARCH ARTICLE

The use of a zwitterionic schiff-base N_2/N_2^{2-} -donor ligand with $CuCl_2$ and $Cu(NO_3)_2$ generates two isostructural square-planar copper(II) complexes that exhibit cytotoxic properties in the low micromolar range.

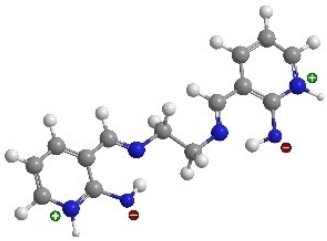

J. Grau, Dr. D. Montpeyó, Dr. J. Lorenzo, Dr. O. Roubeau, Dr. A. Caubet, Prof. P. Gamez**